Theoretical investigation of the behavior of ferroelectric liquid crystals in a magnetic or in a high-frequency electric field

B. Kutnjak-Urbanc
Jožef Stefan Institute, University of Ljubljana, 61111 Ljubljana, Slovenia

B. Žekš
Institute of Biophysics, Medical Faculty, Lipičeva 2, 61105 Ljubljana, Slovenia
(Received 6 December 1991; revised manuscript received 11 February 1993)

A theoretical explanation of the phase diagram of ferroelectric liquid crystals in an external magnetic or high-frequency electric field is given. The investigation is based on a rigorous treatment of the problem within the phenomenological model, being an extension of the Pikin-Indenbom model [Ferroelectrics **20**, 151 (1978)]. The phase transition from the modulated Sm-C^* phase to the homogeneously ordered Sm-C phase is studied numerically. The relevant parameters of the model are chosen in the best way to fit the experimentally obtained critical-field lines on two ferroelectric liquid-crystalline compounds. As a result, the observed relationship between the critical field and the helical pitch in zero field is theoretically confirmed. The critical-field line is investigated in the vicinity of the Lifshitz point where the metastable states appear. In both compounds, the tricritical point is found to be very close to the Lifshitz point, which seems to disagree with measurements showing hysteresis at all temperatures. This contradiction is removed by showing that, in a sample of a finite length along the helical axis, a slow pitch-relaxation process exists. Consequently, during the critical-field measurements, the system is probably not in an equilibrium, which prevents the continuous phase transition from taking place.

PACS number(s): 61.30.Gd, 64.70.Md, 64.70.Rh

I. INTRODUCTION

Among many remarkable properties of the ferroelectric smectic-C^* (Sm-C^*) liquid-crystalline phase, a considerable attention has been paid to the behavior in external magnetic or electric fields [1]. In spite of intensive studies of the behavior in external fields some open questions still remain.

The first theoretical study of the phase diagram of the Sm-C^* liquid crystal under the influence of a magnetic field applied parallel to smectic planes has been done by Michelson [2,3]. Such a system can be, depending on the temperature and on the magnetic field strength, in one of the three phases, in the high-temperature disordered smectic-A (Sm-A) phase, in the modulated Sm-C^* phase, or in the homogeneously tilted Sm-C phase. In the phase diagram in dependence on the temperature T and on the magnetic field strength H, the three phases are separated by three transition lines, Sm-A↔Sm-C^*, Sm-A↔Sm-C, and Sm-C^*↔Sm-C which intersect in the Lifshitz point. Michelson has shown [2] that the wave vector of the modulated Sm-C^* phase goes continuously to zero as we proceed along the Sm-A ↔Sm-C^* transition line towards the Lifshitz point. This feature was later experimentally confirmed by Muševič *et al.* [4] on a sample of p-(n-decyloxy benzylidene)-p-amino-(2-methylbutyl) cinnamate (DOBAMBC). The same group [4,5] has experimentally found the reentrant Sm-C^* phase under the influence of the magnetic field, which is a consequence of a nonmonotonous temperature dependence of the critical magnetic field. The critical magnetic field as a function of temperature has been observed to be related to the temperature dependence of the helical pitch in zero field [5–7]. The anomalous temperature dependence of the pitch and the reentrance of the Sm-C^* phase have remained unexplained within the Pikin-Indenbom model [8] used by Michelson [2]. The critical magnetic field is within this model temperature independent if we neglect the variation of the amplitude of the order parameter, i.e., apply the constant-amplitude approximation (CAA). In the vicinity of the Lifshitz temperature where the CAA is not justified, the critical field is increased due to the variation of the order parameter amplitude.

The first attempt to explain the reentrant Sm-C^* phase in an external magnetic field was made by Jacobs and Benguigui [9,10]. In order to find the critical magnetic field line they had to solve the problem numerically, using the Pikin-Indenbom model extended by two additional terms in the free-energy density. Within the Jacobs-Benguigui model the pitch decreases monotonously with lowering the temperature. Consequently, the critical magnetic field increases by decreasing the temperature within the CAA. However, in the vicinity of the Lifshitz temperature where the variation of the order parameter amplitude is considerable the critical field is increased, leading to the reentrance of the Sm-C^* phase. The Jacobs-Benguigui model does not give any relation between the maximum of the pitch and the reentrant phenomena, although this property has been observed [5,7] in DOBAMBC.

Theoretically both models, the Pikin-Indenbom and the Jacobs-Benguigui model, lead to the continuous phase transition except in the vicinity of the Lifshitz point where the transition Sm-C^*↔Sm-C is of the first order. There is thus a tricritical point on the Sm-C^*↔Sm-C transition line, at which the order of the transition changes. The Jacobs-Benguigui model yields the tricritical point on the critical field line, placed at about the temperature at which the critical-field assumes the minimal value. Experimentally, on the other hand, the tricritical point has not been found. Moreover, most measurements have shown [11,12] a discontinuous character of the transition at all temperatures where the critical field has been measured.

In a previous paper [13] we have proposed the phenomenological model [14–17], which is an extension of the Pikin-Indenbom model, to explain the behavior of ferroelectric liquid crystals in an external magnetic field. The rigorous numerical results have been compared (a) to the results obtained within the CAA and (b) to the rigorous numerical results of the Pikin-Indenbom model. It has been shown that the Pikin-Indenbom model fails to describe the observed critical-field line, except in a narrow temperature regime of the width about 0.1 K. The result obtained within the CAA which gives the critical magnetic field proportional to the inverse pitch in zero field has been found to be valid at practically all temperatures.

The aim of the present paper is to describe the critical magnetic (high-frequency electric) field in dependence on temperature in a way consistent with experimental results. We show that the model used also in our previous paper [13] explains the relationship between the critical field and helical pitch in zero field. We compare the theoretically obtained critical-field line with the measured temperature dependence of the critical field on two ferroelectric liquid-crystalline compounds. The first compound in which the critical magnetic field has been measured is DOBAMBC [4,5]. The other compound is a ferroelectric mixture FCS 101 (Hoffmann La Roche Ltd.) on which the critical high-frequency electric field has been determined [18,19] at field frequencies higher than 10 kHz. As theoretically predicted [20] the phase diagram in the high-frequency electric field is similar to the one in the magnetic field, including the Lifshitz point in which all three phase transition lines intersect. On varying relevant parameters of our model we find the best fit to both experimentally obtained critical-field lines.

We study further the critical-field line in the vicinity of the Lifshitz point and graphically determine the tricritical point. The stability limits of the modulated Sm-C^* phase and the homogeneously ordered Sm-C phase, respectively, are obtained in the regime where the Sm-C^*↔Sm-C phase transition is of the first order. Since the tricritical point appears to be very close to the Lifshitz point, the Sm-C^*↔Sm-C phase transition is expected to be continuous at all temperatures where the critical fields have been measured. This does not agree with most experimental results that show hysteresis and thus a discontinuous character of the transition. We show that this disagreement can be removed by taking into account a finite length of the sample along the helical axis and the phason dynamics in such a system.

The paper is organized as follows. In Sec. II our phenomenological model is introduced and the numerical treatment is described, which leads to the critical magnetic (or high-frequency electric) field line on the phase diagram. All results are presented in Sec. III, where the comparison to experimental data is given and a discontinuous Sm-C^*↔Sm-C phase transition is studied in detail. In Sec. IV the content of the paper is briefly summarized and the observed order of the Sm-C^*↔Sm-C phase transition is discussed in terms of dynamics of finite samples.

II. THE PHENOMENOLOGICAL MODEL

A. Description of the model and its results in zero field

In a Landau description of chiral smectic phases two two-component order parameters are used. A projection of the director to the smectic plane, the tilt $\boldsymbol{\xi} = (\xi_1, \xi_2)$ is used as a primary order parameter and the in-plane polarization $\mathbf{P} = (P_x, P_y)$ as a secondary one, since the latter is induced by the tilt as a consequence of the symmetry. The Pikin-Indenbom model is based on the free-energy density

$$\begin{aligned} f(z) = {} & \frac{a}{2}\left(\xi_1^2+\xi_2^2\right) + \frac{b}{4}\left(\xi_1^2+\xi_2^2\right)^2 - \Lambda\left(\xi_1\frac{d\xi_2}{dz} - \xi_2\frac{d\xi_1}{dz}\right) \\ & + \frac{K_3}{2}\left[\left(\frac{d\xi_1}{dz}\right)^2 + \left(\frac{d\xi_2}{dz}\right)^2\right] \\ & + \frac{1}{2\epsilon}\left(P_x^2+P_y^2\right) - \mu\left(P_x\frac{d\xi_1}{dz} + P_y\frac{d\xi_2}{dz}\right) \\ & + C\left(P_x\xi_2 - P_y\xi_1\right). \end{aligned} \tag{1}$$

The first term in Eq. (1) is the only temperature-dependent term, $a = a_0(T - T_0)$, where T_0 is the critical temperature of the Sm-A↔Sm-C phase transition for the racemic mixture characterized by the absence of all chiral terms. The constants a_0 and b are positive, ensuring the continuity of the Sm-A↔Sm-C^* phase transition in the absence of external fields. The chiral Λ term is the Lifshitz invariant, leading to the helical structure in the Sm-C^* phase and the K_3 term is the elastic term. There are two bilinear coupling terms between both order parameters, the flexoelectric μ term of an achiral origin and the chiral piezoelectric C term. The positive coefficient ϵ denotes the high-temperature dielectric constant. In this model the polarization $\mathbf{P}$ depends linearly upon the tilt $\boldsymbol{\xi}$ and its derivative $d\boldsymbol{\xi}/dz$ along the helical axis z, so that it can be eliminated from Eq. (1). Effectively, the free-energy density, Eq. (1), within the Pikin-Indenbom model reduces to only the first four terms in Eq. (1), where the original constants T_0, Λ, and K_3 are replaced by $\tilde{T}_0 = T_0 + \epsilon C^2/a_0$, $\tilde{\Lambda} = \Lambda + \epsilon\mu C$, and $\tilde{K}_3 = K_3 - \epsilon\mu^2$. The wave vector q_0 corresponding to the helical pitch p_0, $q_0 = 2\pi/p_0$, is temperature independent, $q_0 = \tilde{\Lambda}/\tilde{K}_3$.

Comparing the Pikin-Indenbom model results with experimental data [17] a systematic and qualitative dis-

agreement is found. Therefore it has become necessary to add some invariants of higher order to the free-energy density [Eq. (1)]

$$+\frac{c}{6}\left(\xi_1^2+\xi_2^2\right)^3 - d\left(\xi_1^2+\xi_2^2\right)\left(\xi_1\frac{d\xi_2}{dz}-\xi_2\frac{d\xi_1}{dz}\right)$$

$$+\frac{\eta}{4}\left(P_x^2+P_y^2\right)^2 - \frac{\Omega}{2}\left(P_x\xi_2 - P_y\xi_1\right)^2 \quad (2)$$

and thus to define our phenomenological model [14–17]. The essential point of this model is the presence of an achiral biquadratic coupling [14] (the Ω term) between the tilt $\boldsymbol{\xi}$ and the polarization $\mathbf{P}$ in addition to the bilinear coupling (the C term). Constructing the microscopic model [21] we have shown that the origin of this term is in an additional bipolar ordering of transverse molecular axes, being usually much larger than the polar ordering which leads to the piezoelectric C coupling in the free-energy density [Eq. 1]. This microscopic model also explains the presence of the positive fourth-order term in polarization (the η term) which is of the enthropic origin. In order to describe anomalous temperature dependence of physical quantities (e.g., the pitch of the helix) about 1 K below the critical temperature T_c of the Sm-A↔Sm-C^* phase transition it is sufficient to add only the biquadratic coupling (the Ω term) to the free-energy density [Eq. (1)]. The higher-order Lifshitz term (the d term) accounts for the temperature dependence of the helical pitch p_0 at lower temperatures. The need for the term of the sixth order in the tilt follows from the observed temperature dependence of the specific heat near T_c and its importance has been pointed out independently by Huang and co-workers, Carlsson and Dahl, and Birgeneau *et al.* [22]. Within our model the polarization $\mathbf{P}$ does not depend linearly upon the tilt $\boldsymbol{\xi}$ and its derivative $d\boldsymbol{\xi}/dz$, so that both order parameters appear explicitly in calculation in contrast to the case of the Pikin-Indenbom (PI) model.

We are especially interested in temperature dependence of the wave vector q_0 related to the pitch p_0 in zero field,

$$q_{0,\mathrm{PI}} = \frac{\tilde{\Lambda}}{\tilde{K}_3} \quad \text{and} \quad q_0 = \frac{\Lambda}{K_3} + \frac{\mu}{K_3}\frac{P_0}{\Theta_0} + \frac{d}{K_3}\Theta_0^2, \quad (3)$$

in the Pikin-Indenbom and our model, respectively. The quantities Θ_0 and P_0 are the magnitudes of both order parameters in zero field. In the frame of our model the ratio P_0/Θ_0 sharply increases about 1 K below the critical temperature T_c to an almost constant value at lower temperatures. The wave vector q_0 is a sum of three terms [Eq. (3)], the middle term which includes the ratio P_0/Θ_0 is of an opposite sign to the sign of the first and the third term. Consequently, the wave vector q_0 first decreases with decreasing temperature, reaches a minimum just below T_c, and then increases monotonously as temperature is lowered further. The anomalous behavior below T_c is hidden in the ratio P_0/Θ_0 which strongly depends on the strength of the biquadratic coupling (the Ω term). As the helical period in zero field is $p_0 = 2\pi/q_0$, its temperature dependence is inverted compared to the wave vector dependence.

The Jacobs-Benguigui model [9,10] which also originates in the Pikin-Indenbom model includes the first term of Eq. (2), the c term, and another one which can be shown to be analogous to the d term in Eq. (2) (it differs for a factor and a total derivative from the d term), in addition to the Pikin-Indenbom model terms defined by Eq. (1). In the Jacobs-Benguigui model the polarization $\mathbf{P}$ is still a linear function of the tilt $\boldsymbol{\xi}$ and its derivative $d\boldsymbol{\xi}/dz$, so that only the tilt $\boldsymbol{\xi}$ suffices for a complete description of the system. Due to an absence of the biquadratic coupling, the Jacobs-Benguigui model does not lead to anomalous temperature dependence of physical quantities below T_c and consequently the pitch p_0 decreases monotonously as temperature is lowered.

B. The presence of a magnetic or a high-frequency electric field

If a magnetic field $\mathbf{H}$ is applied perpendicular to the helical axis, $\mathbf{H} = (H, 0)$, the magnetic coupling term should be added to the free-energy density [23]

$$f_H = -\tfrac{1}{2}\chi_a H^2 \xi_1^2, \quad (4)$$

where $\chi_a = \chi_\parallel - \chi_\perp$ denotes the magnetic anisotropy. The magnetic anisotropy is positive, $\chi_a > 0$, in the compound DOBAMBC. In this case the magnetic field tends to align the tilt $\boldsymbol{\xi}$ parallel to the field $\mathbf{H}$.

In an electric field aligned parallel to the y axis, $\mathbf{E} = (0, E)$, two couplings appear in the free-energy density

$$f_E = -EP_y - \tfrac{1}{2}\epsilon_a E^2 \xi_2^2, \quad (5)$$

the former being a linear ferroelectric coupling and the latter is a consequence of a dielectric anisotropy $\epsilon_a = \epsilon_\parallel - \epsilon_\perp$. At very low frequencies of the field and small field strengths the ferroelectric term dominates, whereas at high frequencies (above some ten kHz) the polarization can no longer follow the external field and only the static part of the quadratic term contributes to the response. In this latter case the couplings in Eqs. (4) and (5) have the same form. The phase diagram in the high-frequency electric field is thus similar to the one in the magnetic field as has already been pointed out [20]. In the case of the ferroelectric mixture FCS 101 the anisotropy is slightly negative, $\epsilon_a < 0$, at field frequencies above 10 kHz, for which the phase diagram in the high-frequency electric field has been experimentally determined [18,19]. The high-frequency electric field therefore tends to align the tilt $\boldsymbol{\xi}$ perpendicular to the field $\mathbf{E}$ in this compound. The case of the high-frequency electric field with negative dielectric anisotropy is similar to the case of the magnetic field with negative magnetic anisotropy, if one replaces $\chi_a H^2$ by $\epsilon_a E_0^2/2$ where E_0 is the magnitude of the oscillating field. The case of the negative magnetic anisotropy differs from the case of the positive anisotropy only very close to the critical temperature of the Sm-A↔Sm-C^*

phase transition. The phase diagram for both cases near the Lifshitz point has been studied by Michelson [2,3]. However, at lower temperatures where the CAA is valid both cases lead to the same temperature dependence of the critical field.

In order to understand the behavior of the Sm-C^* phase in a magnetic field, the equilibrium state of the system has to be found in terms of spatial dependences of the order parameters at a given temperature and at a given field. Let us denote the magnitudes of the tilt $\boldsymbol{\xi}$ and the polarization $\mathbf{P}$ by Θ and P, and the phases Φ and $\tilde{\Phi}$ in such a way that $\boldsymbol{\xi} = \Theta(\cos\Phi, \sin\Phi)$ and $\mathbf{P} = P(-\sin\tilde{\Phi}, \cos\tilde{\Phi})$. In the absence of the field the two order parameters are perpendicular, so that $\tilde{\Phi} = \Phi$. In an external magnetic field $\mathbf{H} = (H, 0)$ the equations for two two-component order parameters are obtained by minimization of the free-energy functional. For the magnitude Θ and the phase Φ of the tilt $\boldsymbol{\xi}$ one gets two nonlinear differential equations of the second order, whereas two nonlinear algebraic equations are found for the magnitude P of the polarization and for the phase difference $\Psi = \Phi - \tilde{\Phi}$,

$$
\begin{aligned}
&K_3\Theta'' - \mu P'\sin\Psi - \mu P\Psi'\cos\Psi - a\Theta - b\Theta^3 - c\Theta^5 + 2\Lambda\Theta\Phi' + 4d\Theta^3\Phi' \\
&\qquad - K_3\Theta\Phi'^2 + \mu P\Phi'\cos\Psi + CP\cos\Psi + \Omega\Theta P^2\cos^2\Psi + \chi_a H^2\Theta\cos^2\Phi = 0, \\
&K_3\Theta^2\Phi'' + 2K_3\Theta\Theta'\Phi' - 2\Lambda\Theta\Theta' - 4d\Theta^3\Theta' - \mu\Theta' P\cos\Psi - \mu\Theta P'\cos\Psi \\
&\qquad + \mu\Theta P\Psi'\sin\Psi - \tfrac{1}{2}\chi_a H^2\Theta^2\sin 2\Phi = 0, \qquad (6) \\
&\epsilon^{-1}P + \eta P^3 - \mu\Theta'\sin\Psi - \mu\Theta\Phi'\cos\Psi - C\Theta\cos\Psi - \Omega\Theta^2 P\cos^2\Psi = 0, \\
&-\mu\Theta' P\cos\Psi + \mu\Theta P\Phi'\sin\Psi + C\Theta P\sin\Psi + \tfrac{1}{2}\Omega\Theta^2 P^2\sin 2\Psi = 0.
\end{aligned}
$$

We obtain the previously mentioned CAA solution by keeping constant the magnitudes Θ and P of the two order parameters. This approximation leads to the sine-Gordon equation for the phase Φ of the tilt $\boldsymbol{\xi}$ with the phase difference $\Psi = 0$, similar to the one describing cholesterics in a magnetic field [24]. The solution is of a multisoliton type with the soliton density going continuously to zero as the critical field H_c^{CAA} or $E_{0,c}^{\mathrm{CAA}}$ at which the second-order Sm-C^*↔Sm-C phase transition takes place is approached from below. In this approximation the critical magnetic H_c^{CAA} or critical high-frequency electric field $E_{0,c}^{\mathrm{CAA}}$ is proportional to the wave vector q_0 related to the helical period in zero field p_0, $q_0 = 2\pi/p_0$,

$$
H_c^{\mathrm{CAA}} = \frac{\pi}{2}\sqrt{\frac{K_3}{\chi_a}}q_0, \qquad E_{0,c}^{\mathrm{CAA}} = \frac{\pi}{2}\sqrt{\frac{2K_3}{|\epsilon_a|}}q_0, \qquad (7)
$$

where q_0 is given by Eq. (3).

Close to the Sm-A ↔Sm-C phase transition the CAA is not justified, since the magnitudes of the two order parameters are not constant. Equations (6) have to be solved in a rigorous way. This can only be done numerically. The numerical treatment of Eqs. (6) is similar to the one introduced by Jacobs and Benguigui [9,10]. The only additional difficulty is that in Eqs. (6) the derivatives P' and Ψ' are required, so that one has to include two additional equations for P' and Ψ', which we get by taking derivatives of the last two equations in Eqs. (6). Altogether we have to solve six nonlinear equations, two of them differential, the others algebraic. The procedure is as follows: One linearizes all equations around the trial solution, solves six linear equations, corrects the trial solution, and iterates until the desired accuracy is reached. As an initial approximated solution the solution of the sine-Gordon equation is used for the phase Φ, whereas the amplitudes are taken to be constant and the phase difference $\Psi = 0$.

In order to reduce the number of parameters in our calculation we introduce dimensionless parameters for the temperature t and the magnetic field h or high-frequency electric field e_0,

$$
t = \frac{T_L - T}{T^*}, \qquad h = \frac{H}{H_L}, \qquad e_0 = \frac{E_0}{E_{0,L}}, \qquad (8)
$$

where the Lifshitz temperatures, T_L^+ in the case of positive anisotropy and T_L^- in the case of negative anisotropy, and the Lifshitz fields H_L and $E_{0,L}$ define both Lifshitz points [2],

$$
T_L^+ = \tilde{T}_0 + 4T^*, \qquad H_L = 2\sqrt{\frac{\tilde{\Lambda}^2}{\chi_a\tilde{K}_3}}, \qquad (9)
$$

and

$$T_L^- = \tilde{T}_0, \qquad E_{0,L} = 2\sqrt{\frac{2\tilde{\Lambda}^2}{|\epsilon_a|\tilde{K}_3}}, \tag{10}$$

respectively, where the temperature scale is $T^* = \tilde{\Lambda}^2/a_0\tilde{K}_3$ with renormalized constants $\tilde{T}_0 = T_0 + \epsilon C^2/a_0$, $\tilde{\Lambda} = \Lambda + \epsilon\mu C$ and $\tilde{K}_3 = K_3 - \epsilon\mu^2$. The Jacobs-Benguigui model as well as ours differ from the Pikin-Indenbom model only in some terms of a higher order, which do not affect the Sm-A $\leftrightarrow$Sm-C^* phase transition line. Thus the Lifshitz field and the Lifshitz temperature are the same in all three models.

There are 12 coefficients in our model. The number of adjustable parameters can be reduced by fixing the scales for the coordinate $z^* = \sqrt{c\tilde{K}_3}/b$, for the tilt magnitude $\Theta^* = \sqrt{b/c}$, for the polarization magnitude $P^* = \sqrt{\epsilon b^3}/c$, and for the free-energy density $f^* = b^3/c^2$, so that only six dimensionless parameters remain,

$$\lambda = \frac{\tilde{\Lambda}}{b}\sqrt{\frac{c}{\tilde{K}_3}}, \qquad \delta = \frac{d}{\sqrt{c\tilde{K}_3}}, \qquad \kappa = \frac{\eta\epsilon^2 b^3}{c^2},$$
$$\alpha = \mu\sqrt{\frac{\epsilon}{\tilde{K}_3}}, \qquad \beta = \frac{C\sqrt{c\epsilon}}{b}, \qquad \gamma = \frac{\Omega\epsilon b}{c}. \tag{11}$$

In order to find the critical field h_c or $e_{0,c}$ at a given temperature t, we increase the field h or e_0 until the free energy of the modulated Sm-C^* phase equals the free energy of the homogeneous Sm-C phase. At a given point (h,t) or (e_0,t) on the phase diagram Eqs. (6) have to be solved on a period p using the periodic boundary conditions. The period p enters the calculation as a parameter, so that a minimization of the free energy with respect to p is required. However, this additional minimization is needed only at temperatures t where the Sm-$C^*$$\leftrightarrow$Sm-$C$ transition is discontinuous and the soliton density is finite at the transition. At temperatures t where the transition is expected to be continuous the soliton density at the transition is zero and we only look for a single soliton solution ($p \to \infty$) of Eqs. (6) with fixed asymptotic boundary conditions.

III. RESULTS AND DISCUSSION

A. Comparison to experimental data

In DOBAMBC the critical magnetic field [4,5] H_c and the helical pitch [6] in zero field p_0 have been measured as functions of temperature. The relationship $H_c \propto 1/p_0$ has been tested experimentally [5]. A similar relationship has been noticed also in the compound FCS 101 on which the critical high-frequency electric field $E_{0,c}$ and the helical pitch in zero field p_0 have been determined experimentally in dependence on temperature [18,19].

In the previous paper [13] we have taken the following values of dimensionless parameters given by Eq. (11): $\lambda = -2.4 \times 10^{-2}$, $\delta = -1.27 \times 10^{-2}$, $\kappa = 10$, $\alpha = -5.92 \times 10^{-2}$, $\beta = -8.0 \times 10^{-2}$, and $\gamma = 2.26$. Those values have been obtained by a global analysis [16] of all measured quantities in DOBAMBC.

Here we study the measured critical field and the helical pitch in zero field for each compound separately. We adjust the parameters of our model in order to obtain the best fit to experimental data on the critical field. In a fitting procedure based on the least-squares method only three of the six adjustable parameters given by Eq. (11) are allowed to vary: the parameter δ governing the behavior of the helical pitch p_0 at low temperatures, the parameter γ which accounts for the anomaly in the pitch just below the critical temperature T_c of the Sm-A $\leftrightarrow$Sm-C^* phase transition, and the parameter α which is related to the flexoelectric μ term. Those three parameters influence the temperature dependence of the helical pitch, but the choice is not the only one possible. Due to similar properties of both compounds, all six parameters are expected to remain of about the same order of magnitude, so that to the other three parameters the same values are assumed as in the previous paper [13]. The results of this fitting are in addition to the parameters δ, α, and γ, also the scale for the temperature T^*, the scale for the coordinate z^*, and the Lifshitz field H_L or $E_{0,L}$. As expected also those three parameters which were allowed to change remain of the same order of magnitude as the original values above. It should be mentioned that the temperature dependence of the tilt in zero field is not very sensitive to such small variations of the three parameters which we vary. Moreover, the comparison between the theoretically obtained and the experimentally measured tilt in DOBAMBC shows good agreement.

The results are presented in Fig. 1 for DOBAMBC and in Fig. 2 for FCS 101. On both figures the crosses represent measured [4–6] values of the critical magnetic (in DOBAMBC) or high-frequency electric [18,19] field (in FCS 101). The circles correspond to the inverse values

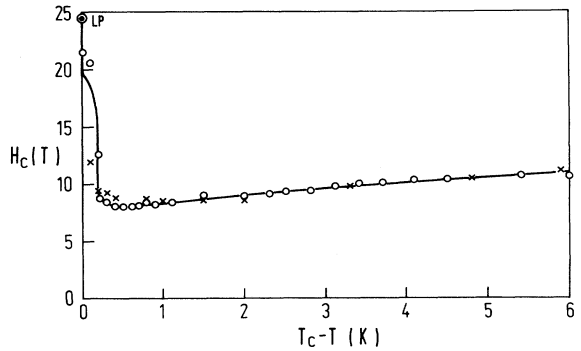

FIG. 1. The critical magnetic field H_c is shown as a function of temperature in DOBAMBC. Crosses correspond to measured values of the critical field, circles to the inverse pitch in zero field, (19.1 Tμm)/p_0, and the solid curve represents the fit with dimensionless parameters $\lambda = -2.40 \times 10^{-2}$, $\delta = -3.16 \times 10^{-3}$, $\kappa = 10$, $\alpha = -3.42 \times 10^{-2}$, $\beta = -8.00 \times 10^{-2}$, and $\gamma = 4.21$. The scales for the coordinate and for the temperature scale are $z^* = 3.79 \times 10^{-3}$ μm and $T^* = 6.65 \times 10^{-4}$ K, whereas the Lifshitz field is equal to $H_L \approx 24.5$ T. LP denotes the Lifshitz point.

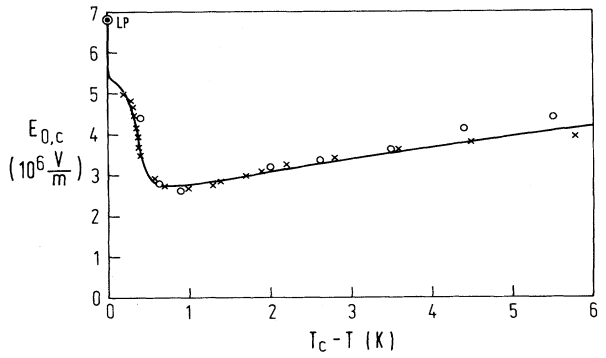

FIG. 2. The critical high-frequency electric field $E_{0,c}$ is shown as a function of temperature in FCS 101. Crosses correspond to measured values of the critical field, circles to the inverse pitch in zero field, 13.2×10^6 V/mμm/p_0, and the solid curve represents the fit with dimensionless parameters $\lambda = -2.40 \times 10^{-2}$, $\delta = -7.25 \times 10^{-3}$, $\kappa = 10$, $\alpha = -3.98 \times 10^{-2}$, $\beta = -8.00 \times 10^{-2}$, and $\gamma = 3.72$. The scales for the coordinate and for the temperature scale are $z^* = 9.44 \times 10^{-3}$ μm and $T^* = 9.87 \times 10^{-4}$ K, whereas the Lifshitz field is equal to $E_{0,L} \approx 6.79 \times 10^6$ V/m.

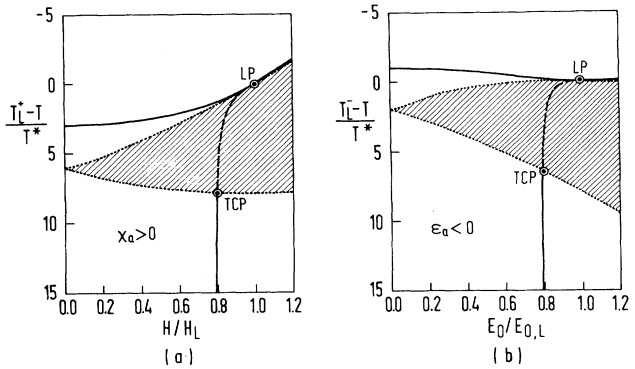

FIG. 3. Determination of the tricritical point (TCP) in both cases, of the positive (a) and of the negative anisotropy (b), based on the analysis of Jacobs and Walker. The hatched area corresponds to temperatures and field strengths for which the interaction between two solitons is attractive. The Sm-C^*↔Sm-C transition line is calculated numerically in both cases.

of the pitch in zero field multiplied by a measured average of the product between the critical field and the pitch in zero field. The solid curves are theoretical curves for the critical fields which coincide with the results of the CAA given by Eqs. (7) almost at all temperatures, except in the very vicinity of the Lifshitz point where experimental data are not available anyway. The difference between the rigorous and the CAA result can be noticed only very close to the Lifshitz point. Here the rigorous critical field increases sharply to the Lifshitz field value, whereas the CAA critical field remains constant, having the value of about $\pi/4$ of the Lifshitz field. This proves our general conclusions [13] about the validity of this approximation. The Pikin-Indenbom model results deviate from results of the presented model at temperatures $T_c - T > 0.1$ K which is also in agreement with the previously reported results [13].

The experimental results in DOBAMBC [5] and in FCS 101 [18,19] show that the product of the critical magnetic (high-frequency electric) field and the helical pitch in zero field is practically temperature independent. The model we use confirms this experimental result. Our results show that at all temperatures where the critical fields have been measured, Eqs. (7) are valid. Thus all the model parameters that influence the pitch in zero field also influence the critical magnetic and high-frequency electric fields in compounds similar to DOBAMBC and FCS 101. The anomaly in the temperature dependence of the helical pitch thus leads to the reentrant Sm-C^* phase in these systems.

B. The regime of a discontinuous Sm-C^*↔ Sm-C phase transition

The determination of the tricritical point is presented graphically in Figs. 3(a) and 3(b) for both cases of positive and negative anisotropy, respectively. The positions of both tricritical points are obtained by using the analysis of Jacobs and Walker [25] who have studied the asymptotic interaction between two solitons in a stable multisoliton solution of Euler-Lagrange equations describing the charge density wave system. The asymptotic behavior which decides about the order of the transition reflects itself in the asymptotic behavior of single soliton solutions at a given point on the critical-field line. Whenever this behavior is pure exponential, the asymptotic interaction is repulsive and the transition is continuous and if it is an exponentially damped sinusoid, this interaction is attractive and the transition discontinuous. The hatched regions in Fig. 3 correspond to temperatures and field strengths at which the asymptotic interaction between two solitons is attractive and the phase transition Sm-C^*↔Sm-C discontinuous.

According to the results of the preceding subsection the temperature scales are in both compounds of the order of $T^* \approx 10^{-3}$ K. Therefore the area where the asymptotic interaction between two solitons is attractive is in DOBAMBC as well as in FCS 101 placed very close to the Lifshitz point. Consequently, the tricritical point is too close to the Lifshitz point to be detected experimentally.

It should be pointed out that the field variation of the Sm-A ↔Sm-C^* phase transition temperature as well depends on the temperature scale T^*. In the case of DOBAMBC and FCS 101 the scale is so small that this dependence is very weak, $T_L \approx T_c$, where T_c is the Sm-A ↔Sm-C^* transition temperature in zero field. However, there are such compounds (e.g., CE-8) where the temperature scale T^* is expected to be much larger [12] and consequently the dependence of the Sm-A ↔Sm-C^* phase transition temperature on the field stronger. In such systems the tricritical point itself would be shifted to lower temperatures where it could in principle be detected.

For compounds similar to DOBAMBC and to FCS 101 the whole range of the first-order Sm-C^*↔Sm-C transi-

tion is in the temperature regime where the magnitudes of both order parameters are small, so that the additional terms of higher order given by Eq. (2) can be neglected. The properties of the system in the vicinity of the tricritical point can be studied within the Pikin-Indenbom model, defined by the free-energy density expansion, Eq. (1). In the following the behavior near the tricritical point is considered only in the case of positive magnetic anisotropy, in the other case the behavior is expected to be similar.

In Fig. 4 three lines $h_c^-(t)$, $h_c(t)$, and $h_c^+(t)$ are depicted in the regime where the Sm-C^*↔Sm-C phase transition is discontinuous. The critical line $h_c^-(t)$ represents the stability line of the homogeneous Sm-C phase, along which the free energy of the single soliton solution equals the free energy of the homogeneous state, and the critical line $h_c^+(t)$ is the stability limit of the modulated Sm-C^* phase. The critical field line $h_c(t)$ between the two stability limits is the line along which the free energy of the equilibrium soliton lattice is equal to the free energy of the homogeneous state. Metastable states appear at fields and temperatures between the two stability limits. As the free energies are analytic functions near the Lifshitz point and near the tricritical point, the three critical lines are expected to intersect with common tangents in those two points. At a given temperature the differences between the fields h_c^-, h_c, and h_c^+, as seen from Fig. 4, are of the order of a few percent. In the following we show how the stability limit $h_c^+(t)$ and the critical-field line $h_c(t)$ can be determined.

At a given point (h,t) on the phase diagram an average free-energy density f_{av} can be defined

$$f_{av} = \frac{1}{L}\int_{-\frac{L}{2}}^{+\frac{L}{2}} [f(z) - f_c]\, dz, \tag{12}$$

where f is a free-energy density of the modulated Sm-C^* phase, Eq. (1), $f_c = -(\tilde{a} - \chi_a H^2)^2/4$ is the free-energy density of the homogeneous Sm-C phase, and $\tilde{a} = a_0(T - \tilde{T}_0)$. The average free-energy density, Eq. (12), is still a function of the period L on which the multisoliton solution is obtained. The period L is defined by the relationship $\Phi(z + L) = \pi + \Phi(z)$. In Figs. 5(a) and 5(b) the average free-energy density in dimensionless form $\bar{f} = f_{av}/f_0$ (where $f_0 = \tilde{\Lambda}^4/b\tilde{K}_3^2$) is depicted as a function of a wave vector normalized to the wave vector $q_0 = 2\pi/p_0$ in zero field, $q = p_0/2L$, for different values of the field h. Figure 5(a) indicates the wave vector dependence of $\bar{f}$ for the temperature $t = 2$ in the regime of the first-order transition. It can be seen that the minimum of $\bar{f}$ at a finite $q \neq 0$ is getting less pronounced by increasing the field from $h < h_c^-$ to $h = h_c^+$ where it disappears. Due to the presence of a metastable state in the region $h_c^- < h < h_c^+$, there are always two minima of $\bar{f}$, one at $q = 0$ and the other at $q \neq 0$. Figure 5(b) refers to the temperature $t = 10$ at which the Sm-C^*↔Sm-C

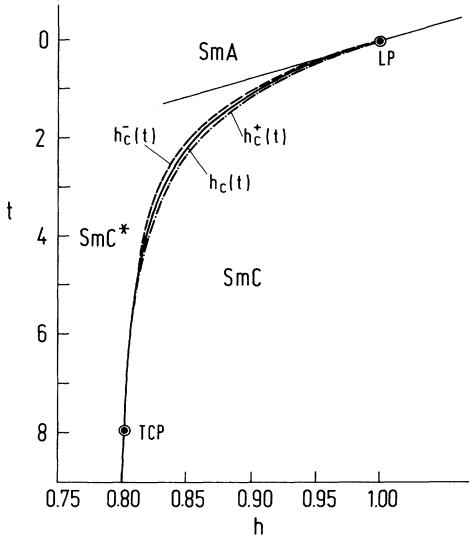

FIG. 4. The phase diagram in an external magnetic field near the Sm-A ↔Sm-C^* transition line for the case of the positive anisotropy calculated on the basis of the Pikin-Indenbom model. The three critical lines $h_c^-(t)$, $h_c(t)$, and $h_c^+(t)$ are shown to intersect in the Lifshitz point and in the tricritical point. The metastable states exist between the stability lines $h_c^-(t)$ and $h_c^+(t)$.

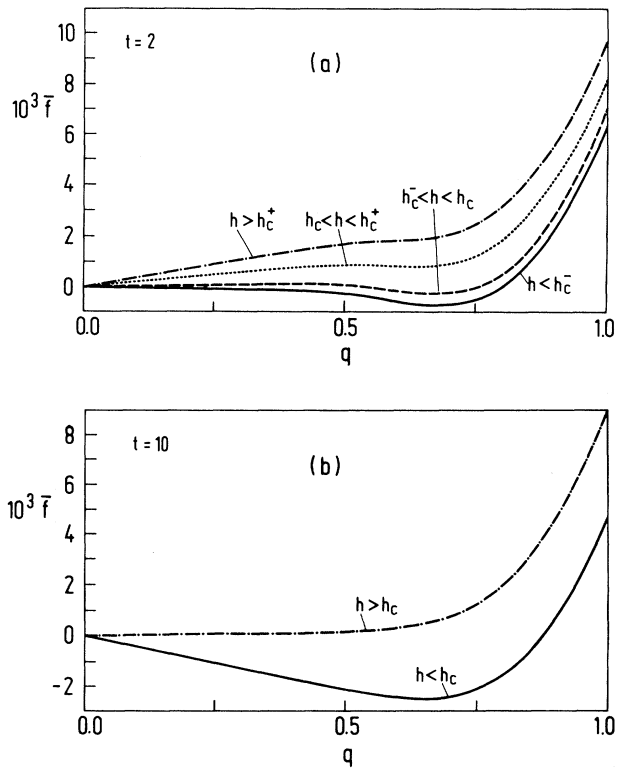

FIG. 5. The normalized average free-energy density $\bar{f} = f_{av}/f_0$ (where $f_0 = \tilde{\Lambda}^4/b\tilde{K}_3^2$) is depicted as a function of the wave vector q at two different reduced temperatures, (a) $t = 2$ and (b) $t = 10$. In the case (a) the Sm-C^*↔Sm-C phase transition is discontinuous and the four curves correspond to four different reduced fields increasing from $h < h_c^-$ to $h > h_c^+$. For fields $h \in [h_c^-, h_c^+]$ $\bar{f}$ obtains two minima, whereas for fields outside this region where the transition is continuous $\bar{f}$ has only one minimum as in the case (b).

transition is continuous. There is only one stable state in this regime, so that the average free-energy density $\bar{f}$ has only one minimum in both cases, $h < h_c$ and $h > h_c$. By increasing the field from $h < h_c$ the minimum at $q \neq 0$ moves to smaller wave vectors and continuously transforms into the minimum at $q = 0$ when $h = h_c$. The equilibrium state is determined by the wave vector q at which the average free-energy density is minimal. The equilibrium wave vector $q = p_0/2L$ is presented in Fig. 6 as a function of the field h at the reduced temperature $t = 2$. The limits of stability h_c^- and h_c^+ are designated as well.

The CAA breaks down in the vicinity of the Lifshitz point, at about $t < 20$. We are interested in the behavior of the critical field h_c^{CAA} obtained on the basis of this approximation in comparison to the rigorous critical field value h_c at reduced temperatures $t \in (10, 200)$. On this temperature interval the transition is continuous and the Pikin-Indenbom model is appropriate. One can find out analytically how the result of the CAA approaches the rigorous result when the temperature is lowered, i.e., the reduced temperature t is increased. It can be shown that the relative difference between the exact H_c and the approximated critical field H_c^{CAA}, $\Delta H_c/H_c = (H_c - H_c^{\mathrm{CAA}})/H_c$, behaves as

$$\frac{\Delta H_c}{H_c} \propto \frac{1}{T_c - T}, \tag{13}$$

at low temperatures T. This result has been confirmed numerically as well. According to the temperature scale for the two compounds considered in the preceding subsection the analytically predicted relationship, Eq. (13), is valid at temperatures T for which $T_c - T > 0.01$ K. At $T_c - T = 0.01$ K the relative critical-field difference

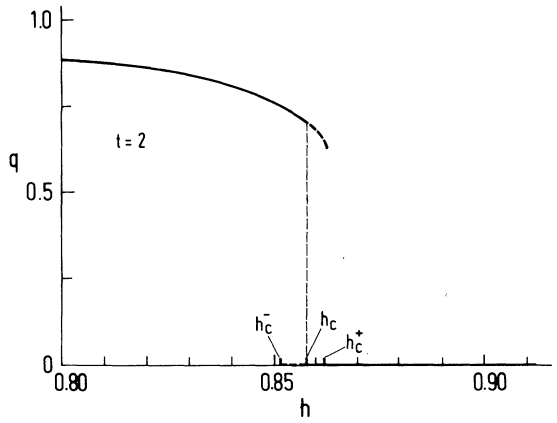

FIG. 6. The wave vector q of the pitch within the Pikin-Indenbom model is presented at fixed reduced temperature $t = 2$ as a function of the reduced field in the case of the positive anisotropy. The jump of q occurs at $h = h_c$. The limits of stability h_c^- and h_c^+ are marked. For reduced fields $h \in [h_c^-, h_c]$ the metastable state is the homogeneous state with $q = 0$, whereas the stable state is a modulated state with $q \neq 0$. For reduced fields $h \in [h_c, h_c^+]$ the situation is reversed. The two dashed curves between h_c^- and h_c and between h_c and h_c^+ represent the metastable states.

is about $\Delta H_c/H_c \approx 0.01$ and at lower temperatures T it decreases as $(T_c - T)^{-1}$. The CAA is therefore valid at all temperatures $T_c - T > 0.01$ K. The temperature interval where the CAA is valid again depends on the temperature scale T^*. However, its validity in a particular system can only be determined numerically by comparing the CAA and rigorous numerical results.

IV. CONCLUSIONS

To summarize, we have studied theoretically the Sm-C^*↔Sm-C phase transition induced either by a magnetic or a high-frequency electric field on the basis of the phenomenological model which is an extension of the Pikin-Indenbom model. Our aim was to explain theoretically the phase diagram in the magnetic (high-frequency electric) field consistently with experimental findings [5,18,19].

The reentrant behavior of ferroelectric liquid crystals has been investigated for the first time [9,10] by Jacobs and Benguigui. Within the constant-amplitude approximation their model yields the critical magnetic field which increases monotonously on lowering the temperature. In the vicinity of the Lifshitz point where the magnitudes of both order parameters are not constant the critical field is increased compared to the CAA value, so that the critical-field line becomes nonmonotonous, leading to the reentrant behavior. Within their model there is no relation between the maximum of the pitch and the reentrant phenomenon, which does not agree with experimental results [5,18,19]. The Jacobs-Benguigui model is appropriate to describe the critical magnetic field in compounds [26] in which the helical pitch decreases monotonously on lowering temperature. The minimum of the critical magnetic field in these systems and thus the reentrance of the Sm-C^* phase would appear close to the Lifshitz temperature where the constant-amplitude approximation is not valid. Unfortunately, measurements of the critical magnetic field in such systems are not available.

The model we use comprises the Jacobs-Benguigui model as a special case and accounts also for more realistic systems with an anomalous temperature dependence of the pitch [6,19] and other physical quantities. It leads to the reentrant behavior of the Sm-C^* phase already within the constant-amplitude approximation. The critical magnetic (high-frequency electric) field is found to be inversely proportional to the helical pitch in zero field, confirming the experimental findings [5,18,19] in DOBAMBC and FCS 101. The relationship between the critical field and helical pitch breaks down only very close to the Lifshitz temperature T_L, $T_L - T < 10^{-2}$ K, where the critical field has not been measured anyway.

In this paper the comparison of the theoretical results to experimental data has been done. The model parameters have been adjusted to give the best fit to measured data on two ferroelectric liquid-crystalline compounds, in DOBAMBC and in the mixture FCS 101. Our analysis shows that the nonmonotonous temperature dependence of the critical magnetic or high-frequency electric

field is in these compounds directly related to the anomalous temperature dependence of the helical pitch in zero field, since the CAA results given by Eqs. (7) are valid at practically all temperatures where the critical fields have been measured. The minimum of the critical field at about $T_L - T \approx 1$ K thus corresponds to the maximum of the helical pitch in both compounds [5,18,19]. On the other hand, the validity of the Pikin-Indenbom model is restricted to a narrow temperature interval below the Lifshitz point, $T_L - T < 0.1$ K. Due to a small temperature scale, $T^* \approx 10^{-3}$ K, the critical temperature T_c of the Sm-A $\leftrightarrow$Sm-C^* phase transition is practically field independent, i.e., $T_c \approx T_L$.

The tricritical point in both samples has been found to be so close to the Lifshitz point that in the temperature regime where measurements are mostly done the Sm-$C^*\leftrightarrow$Sm-C phase transition should be continuous. However, most experiments performed on samples in the bookshelf geometry [11] show a discontinuous character of the transition, although in the case of the homeotropic geometry a continuous transition is possible [12]. This discrepancy can be understood by considering the dynamics in finite samples. The zero field relaxation rate of the dynamical process which corresponds to the relaxation of the helical period is expected to be very low. Its relaxation frequency in a finite sample can be estimated within the CAA. We denote the sample length along the helical axis by d and assume that at both boundaries the molecular director is free to rotate on the smectic cone. We look for such a dynamical process which changes the length of the helical pitch and costs the least energy. The phason dynamics in zero field is usually presented by the phase fluctuation spectrum [27], showing the inverse relaxation time $\tau_{\rm ph}^{-1}$ in dependence on the wave vector q, $\tau_{\rm ph}^{-1} = \gamma^{-1}K_3(q - q_0)^2$. Here γ is the rotational viscosity and q_0 is the critical wave vector related to the helical period p_0 in zero field, $q_0 = 2\pi/p_0$. The phason mode at the critical wave vector q_0 corresponds to the rotation of the helix as a whole and it costs no energy. The phase fluctuation we are looking at has a wavelength $\lambda = 2d$ and is associated with the phason mode at $q = q_0 \pm \pi/d$, so that the inverse relaxation time equals $\tau_{\rm relax}^{-1} = \gamma^{-1}K_3(\pi/d)^2$. The relaxation time $\tau_{\rm relax}$ can be expressed in terms of the Goldstone mode frequency $f_G = [2\pi\tau_{\rm ph}(q = 0)]^{-1} = (2\pi\gamma)^{-1}K_3q_0^2$, which can be determined by dielectric measurements, as

$$\tau_{\rm relax} = \frac{1}{2\pi f_G}\left(\frac{d}{p_0}\right)^2 .$$

The relaxation time is proportional to the square of the sample thickness d and can be quite long in thick samples. This result is similar to the one obtained by a more detailed analysis on cholesterics [28]. Using typical values for the helical period [4] $p_0 \approx 1$ μm and for the Goldstone mode frequency [29] ranging from 100 Hz to 1 kHz, one can estimate $\tau_{\rm relax}$ in the homeotropic geometry, where $d \approx 100$ μm represents the sample thickness between the plates, and in the bookshelf geometry, respectively, where $d \approx 1$ cm is a linear dimension along the electrodes. In the former case $\tau_{\rm relax}^h$ assumes the values from a few tenths of a second to a few seconds and in the latter case $\tau_{\rm relax}^b$ ranges from a few minutes to few hours ($\tau_{\rm relax}^b \approx 10^4\ \tau_{\rm relax}^h$). Especially in the case of the bookshelf geometry this relaxation time is long compared to the time in which the critical field is normally measured. Consequently, the observed first-order character of the Sm-$C^*\leftrightarrow$Sm-C phase transition might be a result of the fact that during the experiment the system is not in equilibrium.

[1] L. Lam and J. Prost, *Solitons in Liquid Crystals* (Springer-Verlag, New York, 1992), Chap. 10.
[2] A. Michelson, Phys. Rev. Lett. **39**, 464 (1977).
[3] A. Michelson, Phys. Rev. B **16**, 577 (1977).
[4] I. Muševič, B. Žekš, R. Blinc, Th. Rasing, and P. Wyder, Phys. Rev. Lett. **48**, 192 (1982).
[5] R. Blinc, I. Muševič, B. Žekš, and A. Seppen, Phys. Scr. **T35**, 38 (1991).
[6] I. Muševič, B. Žekš, R. Blinc, L. Jansen, A. Seppen, and P. Wyder, Ferroelectrics **58**, 71 (1984).
[7] A. Seppen, Ph.D. thesis, University of Nijmegen, 1987.
[8] V. L. Indenbom, S. A. Pikin, E. B. Loginov, Kristallografiya **21**, 1093 (1976) [Sov. Phys. Crystallogr. **21**, 632 (1976)]; S.A. Pikin and V.L. Indenbom, Ferroelectrics **20**, 151 (1978).
[9] L. Benguigui and A. E. Jacobs, Ferroelectrics **84**, 379 (1988).
[10] A. E. Jacobs and L. Benguigui, Phys. Rev. A **39**, 3622 (1989).
[11] I. Muševič, B. Žekš, R. Blinc, Th. Rasing, and P. Wyder, Phys. Status Solidi B **119**, 727 (1983).
[12] I. Muševič (personal communication).
[13] B. Kutnjak-Urbanc and B. Žekš, in *Phase Transitions in Liquid Crystals*, edited by S. Martellucci and A. N. Chester (Plenum, New York, 1992), Chap. 23.
[14] B. Žekš, Mol. Cryst. Liq. Cryst. **114**, 259 (1984).
[15] S. Dumrongrattana and C. C. Huang, Phys. Rev. Lett. **56**, 464 (1986).
[16] T. Carlsson, B. Žekš, C. Filipič, A. Levstik, and R. Blinc, Mol. Cryst. Liq. Cryst. **163**, 11 (1988).
[17] B. Žekš, T. Carlsson, C. Filipič, and B. Urbanc, Ferroelectrics **84**, 3 (1988).
[18] Z. M. Sun, X. Zhang, and D. Feng, Europhys. Lett. **11**, 415 (1990).
[19] Z. H. Wang, Z. M. Sun, and D. Feng, Europhys. Lett. **14**, 785 (1991).
[20] R. Blinc and F.C. de Sa Barreto, Phys. Status Solidi B **87**, K105 (1978).
[21] B. Urbanc and B. Žekš, Liq. Cryst. **5**, 1075 (1989); B. Žekš and B. Urbanc, Ferroelectrics **84**, 3 (1991).
[22] C. C. Huang and J. M. Viner, Phys. Rev. A **25**, 3385 (1982); T. Carlsson and I. Dahl, Mol. Cryst. Liq. Cryst.

95, 373 (1983); S. Dumrongrattana, G. Nounesis, and C. C. Huang, Phys. Rev. A **33**, 2181 (1986); R. J. Birgeneau, C. W. Garland, A. R. Kortan, J. D. Litster, M. Meichle, B. M. Ocko, C. Rosenblatt, L. J. Yu, and J. Goodby, Phys. Rev. A **27**, 1251 (1983).

[23] P.G. de Gennes, *Physics of Liquid Crystals* (Oxford University Press, Belfast, 1974).

[24] P. G. de Gennes, Solid State Commun. **6**, 163 (1968).

[25] A. E. Jacobs and M. B. Walker, Phys. Rev. B **21**, 4132 (1980).

[26] J. Li, H. Takezoe, and A. Fukuda, Jpn. J. Appl. Phys. **30**, 532 (1991).

[27] I. Muševič, R. Blinc, B. Žekš, C. Filipič, T. Čopič, A. Seppen, P. Wyder, and A. Levanyuk, Phys. Rev. Lett. **60**, 1530 (1988).

[28] R. M. Hornreich and S. Shtrikman, Phys. Rev. A **44**, 3430 (1991).

[29] A. Levstik, B. Žekš, I. Levstik, R. Blinc, and C. Filipič, J. Phys. C **40**, 303 (1979).